



Published in final edited form as:

*Circ Arrhythm Electrophysiol.* 2013 October ; 6(5): 960–966. doi:10.1161/CIRCEP.113.000439.

## Selective Targeting of Gain-of-function KCNQ1 Mutations Predisposing to Atrial Fibrillation

Courtney M. Campbell, BA, MA<sup>1</sup>, Jonathan D. Campbell, BS<sup>2</sup>, Christopher H. Thompson, PhD<sup>3</sup>, Carlos G. Vanoye, PhD<sup>3</sup>, and Alfred L. George Jr., MD<sup>1,3</sup>

<sup>1</sup>Department of Pharmacology, Vanderbilt University, Nashville, TN

<sup>2</sup>Department of Engineering Management, Information, and Systems, Southern Methodist University, Dallas, TX

<sup>3</sup>Division of Genetic Medicine, Department of Medicine, Vanderbilt University, Nashville, TN

### Abstract

**Background**—Atrial fibrillation (AF) is the most common sustained cardiac arrhythmia in adults. We hypothesized that gain-of-function KCNQ1 mutations previously associated with familial AF have distinct pharmacological properties that may enable targeted inhibition.

**Methods and Results**—Wild-type (WT) KCNQ1 or the familial AF mutation KCNQ1-S140G were heterologously co-expressed with KCNE1 to enable electrophysiological recording of the slow delayed rectifier current ( $I_{Ks}$ ) and investigation of pharmacological effects of the  $I_{Ks}$  selective blocker HMR-1556. Co-expression of KCNQ1-S140G with KCNE1 generated potassium currents (S140G- $I_{Ks}$ ) that exhibited greater sensitivity to HMR-1556 than WT- $I_{Ks}$ . Enhanced HMR-1556 sensitivity was also observed for another gain-of-function AF mutation, KCNQ1-V141M. Heteromeric expression of KCNE1 with both KCNQ1-WT and KCNQ1-S140G generated currents (HET- $I_{Ks}$ ) with gain-of-function features including larger amplitude, a constitutively active component, hyperpolarized voltage dependence of activation, and extremely slow deactivation. A low concentration of HMR-1556, which had little effect on WT- $I_{Ks}$  but was capable of inhibiting the mutant channel, reduced both instantaneous and steady-state HET- $I_{Ks}$  to levels that were not significantly different from WT- $I_{Ks}$  and attenuated use-dependent accumulation of the current. In cultured adult rabbit left atrial myocytes, expression of S140G- $I_{Ks}$  shortened action potential duration (APD) compared to WT- $I_{Ks}$ . Application of HMR-1556 mitigated S140G- $I_{Ks}$ -induced APD shortening and did not alter APD in cells expressing WT- $I_{Ks}$ .

**Conclusions**—The enhanced sensitivity of KCNQ1 gain-of-function mutations for HMR-1556 suggests the possibility of selective therapeutic targeting and, therefore, our data illustrates a potential proof-of-principal for genotype-specific treatment of this heritable arrhythmia.

### Keywords

arrhythmia; atrial fibrillation; antiarrhythmic drug; potassium channels; genetics

### Introduction

Atrial fibrillation (AF) is the most common cardiac arrhythmia in adults. The prevalence of AF rises exponentially with age, and because of the aging population, the number of persons

Correspondence: Alfred L. George, Jr., M.D., Division of Genetic Medicine, Vanderbilt University, 529 Light Hall, 2215 Garland Ave., Nashville, TN 37232-0275, Tel: 615-936-2660, Fax: 615-936-2661, al.george@vanderbilt.edu.

**Conflict of Interest Disclosures:** None.

with AF in the United States is projected to increase to 12 million by 2050.<sup>1</sup> Importantly, AF confers a 6-fold increased risk for thromboembolic disease including stroke, predisposes to heart failure and is associated with premature death.<sup>2</sup> The incremental healthcare costs directly related to the diagnosis and management of AF in the United States have been estimated at \$6 billion.<sup>3</sup>

Most often, AF occurs within the context of structural heart disease with onset past the age of 65 years. However, an estimated 10–30% of AF, designated as lone AF, arises in the absence of overt heart disease and has a younger age of onset.<sup>4–7</sup> Genetic predisposition to AF has been demonstrated in populations<sup>8,9</sup> and in families with monogenic forms of the disease.<sup>10</sup> AF-associated mutations have been identified in potassium channels,<sup>11–16</sup> sodium channels,<sup>17–19</sup> and other genes.<sup>20</sup> The mutation KCNQ1-S140G was the first identified mutation and remains the best-studied genetic variant associated with autosomal dominant AF.<sup>11,21–23</sup>

KCNQ1 encodes a pore-forming voltage-gated potassium channel (Kv7.1 or KCNQ1) that combines with the auxiliary subunit KCNE1 to generate the slow component of the delayed rectifier potassium current ( $I_{Ks}$ ), critical for cardiac action potential repolarization. Co-expression of KCNQ1-S140G with KCNE1 (S140G- $I_{Ks}$ ) demonstrated a gain-of-function with larger and more instantaneous current activation.<sup>11,23</sup> A similar gain-of-function effect occurs with the AF-associated mutation KCNQ1-V141M.<sup>12</sup> These *in vitro* data are consistent with the notion that increased repolarizing potassium current evoked by these mutations cause shortening of atrial action potentials in myocytes and an abbreviated effective refractory period in atrial tissues, resulting in an increased probability of reentry circuits and AF.<sup>23</sup>

We hypothesized that KCNQ1 gain-of-function mutations have pharmacological properties distinct from the WT channel that may enable selective inhibition of mutant channel complexes. Pharmacological targeting of this gain-of-function behavior would be predicted to decrease AF susceptibility in persons with this dominant mutant allele. We tested this hypothesis using the chromanol 293B derivative HMR-1556, a highly specific  $I_{Ks}$  blocker when used at low concentrations. Here we present evidence that S140G- $I_{Ks}$  and V141M- $I_{Ks}$  exhibit enhanced sensitivity to HMR-1556 due to an additional high affinity state. Using a concentration that predominantly inhibits the high affinity state, HMR-1556 effectively suppressed S140G- $I_{Ks}$  amplitudes to levels not different from WT- $I_{Ks}$ , attenuated the use-dependent accumulation of current without significant effects on WT- $I_{Ks}$ , and mitigated action potential shortening in cultured adult rabbit left atrial myocytes without affecting WT- $I_{Ks}$  action potential duration. These data suggest a potential opportunity for genotype-specific treatment of familial AF.

## Methods

Voltage clamp experiments were performed in Chinese hamster ovary (CHO) cells transiently transfected with plasmids containing potassium channel subunits (KCNQ1, KCNE1) constructed in plasmids co-expressing a transfection marker (dsRedMST, eGFP, or CD8). Recordings were done in the absence or presence of HMR-1556. Current clamp recordings were performed with cultured adult rabbit left atrial myocytes infected with adenoviruses encoding WT or mutant KCNQ1 subunits in combination with a separate adenovirus encoding KCNE1. Action potentials were elicited from transduced myocytes using whole cell patch clamp 48–72 hours post-isolation in the absence or presence of HMR-1556.

Differences between two groups were assessed using unpaired Student's *t* test. When comparing more than two groups, one-way ANOVA followed by a Tukey post hoc test was performed on values obtained for a given membrane voltage. Statistical tests were performed using SigmaStat 2.03 (Systat Software, Inc., Chicago, IL). Significance levels are reported as two-sided *p*-values.

A complete description of all experimental methods is presented in the Supplementary Material.

## Results

### S140G-I<sub>Ks</sub> exhibits enhanced sensitivity to HMR-1556

We tested whether heterologously expressed I<sub>Ks</sub> channel complexes consisting of either wildtype (WT) or mutant (S140G) KCNQ1 subunits in combination with the auxiliary subunit KCNE1 are inhibited by HMR-1556. Whole-cell recordings of CHO cells transfected with S140G and KCNE1 (S140G-I<sub>Ks</sub>) demonstrated nearly instantaneous activation of outward current in contrast to the slowly activating current observed in cells expressing WT-I<sub>Ks</sub> (Figure 1A, B). Because KCNQ1-S140G mutation-positive subjects were reported to be heterozygous in familial AF and because WT and mutant KCNQ1 subunits can co-assemble in heteromeric channels, we examined channel complexes consisting of both WT and mutant subunits co-expressed with KCNE1 (HET-I<sub>Ks</sub>), which exhibited larger amplitudes with a large fraction of instantaneous current (Figure 1C). Superfusion of 1 μM HMR-1556 completely and rapidly inhibited all channel complexes activated by low frequency pulsing (10 s interpulse duration) to +40 mV (Figure 1D–F). However, inhibition of S140G-I<sub>Ks</sub> and HET-I<sub>Ks</sub> was more pronounced than WT-I<sub>Ks</sub> at lower concentrations.

We assessed concentration-response relationships for WT-I<sub>Ks</sub>, S140G-I<sub>Ks</sub>, and HET-I<sub>Ks</sub> to determine whether the channel complexes have different affinities for HMR-1556 (Figure 2). Cells expressing WT-I<sub>Ks</sub> exhibited a concentration-response curve that was fit by the Hill equation yielding an IC<sub>50</sub> of 214 nM and Hill coefficient of 1.2. By contrast, S140G-I<sub>Ks</sub> exhibited a complex concentration-response that suggested two affinity states. The IC<sub>50</sub> of the high affinity state was 3.7 nM, whereas the lower affinity state had an IC<sub>50</sub> of 97.7 nM. Both states were significantly different from the IC<sub>50</sub> for WT-I<sub>Ks</sub> (*p*<0.001). Hill coefficients for the high (2.2) and low (2.5) affinity states on S140G-I<sub>Ks</sub> suggested positive cooperative binding of the drug. The gating kinetics of the current sensitive to 30 nM HMR-1556, a concentration near the crux between the two affinity states on the concentration-response curve, was not overtly different than drug-insensitive current (Figure S1) suggesting that the two affinity states do not emerge from distinct populations of channels. The HET-I<sub>Ks</sub> complex demonstrated an intermediate pharmacologic phenotype with a complex concentration-response curve. The high affinity state had an IC<sub>50</sub> of 5.1 nM (Hill coefficient 1.7) whereas the low affinity state IC<sub>50</sub> was 240 nM (Hill coefficient 2.4).

There were also substantial differences in the kinetics of HMR-1556 inhibition. Specifically, on- and off-rates observed for suppression of S140G-I<sub>Ks</sub> were significantly slower than WT-I<sub>Ks</sub> (Figure S2). The dramatically slower off-rate for S140G-I<sub>Ks</sub> suggested a stronger interaction between HMR-1556 and the channel consistent with our finding that the mutant subunit confers an enhanced affinity for the drug. The intermediate phenotype of HET-I<sub>Ks</sub> exhibited an on-rate comparable to WT-I<sub>Ks</sub> but a significantly slower off-rate that was more similar to S140G-I<sub>Ks</sub>. This enhanced sensitivity suggested an opportunity to selectively suppress the mutant current with minimal effects on WT-I<sub>Ks</sub>.

### V141M-I<sub>Ks</sub> exhibits enhanced sensitivity to HMR-1556

We also determined the pharmacologic effects of HMR-1556 on another previously reported gain-of-function KCNQ1 mutation, V141M, associated with early onset AF.<sup>12</sup> V141M-I<sub>Ks</sub> exhibited enhanced sensitivity to HMR-1556 and a complex IC<sub>50</sub> binding curve with values similar to S140G-I<sub>Ks</sub> (Figure 3). The off-rate was significantly slower than WT-I<sub>Ks</sub> (Figure S2). These data demonstrate that increased HMR-1556 sensitivity was not specific to S140G-I<sub>Ks</sub>. All further experiments were conducted with S140G-I<sub>Ks</sub> as a prototypic familial AF mutation.

### Properties of heteromeric S140G-I<sub>Ks</sub> and WT-I<sub>Ks</sub>

We elucidated the functional properties of HET-I<sub>Ks</sub>. Compared to WT-I<sub>Ks</sub>, cells expressing HET-I<sub>Ks</sub> exhibited larger amplitudes with a large fraction of instantaneous current between -80 and -20 mV (Figure S3). At more positive voltage steps (-20 to +60 mV), HET-I<sub>Ks</sub> exhibits both time-dependent and constitutive activation with significantly greater current density than WT-I<sub>Ks</sub> (Figure S3). The voltage dependence of activation was shifted significantly in the hyperpolarized direction for HET-I<sub>Ks</sub> ( $V_{1/2}$ : HET-I<sub>Ks</sub>, 1.4±8.1 mV; WT-I<sub>Ks</sub>, 30.1±9.3 mV;  $p < 0.001$ ) without any difference in slope factor (Figure S3). The time course of deactivation was extremely slow for HET-I<sub>Ks</sub> as compared to WT-I<sub>Ks</sub> (Figure S3).

During repetitive depolarization to +40 mV with a short recovery period, both WT-I<sub>Ks</sub> and HET-I<sub>Ks</sub> exhibited a use-dependent accumulation of instantaneous and steady-state current over time, but HET-I<sub>Ks</sub> current density was significantly greater than WT-I<sub>Ks</sub> at each successive pulse (Figure S4). The ratio of instantaneous to steady-state current at the end of this protocol, a proxy for the degree of constitutive activation, was much greater for HET-I<sub>Ks</sub> (84±3%) than WT-I<sub>Ks</sub> (38±4%;  $p < 0.001$ ). These findings illustrate the dynamic nature of I<sub>Ks</sub> and further emphasize the biophysical consequences of the gain-of-function mutation, KCNQ1-S140G.

### Selective inhibition of HET-I<sub>Ks</sub> with HMR-1556

Given the enhanced sensitivity of S140G-I<sub>Ks</sub> to HMR-1556, we hypothesized that HET-I<sub>Ks</sub> could be selectively suppressed by using a concentration HMR-1556 that predominantly inhibits the high affinity state. To test this hypothesis, we applied 20nM HMR-1556 or vehicle to heterologously expressed channels and assessed the effects of drug on gating kinetics and current amplitudes.

Vehicle had no effects on the behavior of WT-I<sub>Ks</sub> and HET-I<sub>Ks</sub> (Figure 4A,B). Further, 20nM HMR-1556 had no appreciable effect on current levels or gating behavior of WT-I<sub>Ks</sub> (Figure 4C), but the drug exerted notable effects on HET-I<sub>Ks</sub> including suppression of both instantaneous and steady-state current amplitude and attenuation of use-dependent current accumulation (Figure 4D). The effects of 20nM HMR-1556 on WT-I<sub>Ks</sub> and HET-I<sub>Ks</sub> are quantified in Figure 5A–D. Importantly, 20nM HMR-1556 did not inhibit WT-I<sub>Ks</sub>, but did reduce the amplitude of HET-I<sub>Ks</sub> to levels that were not significantly different ( $p = 0.32$ ) from WT-I<sub>Ks</sub>. Additionally, the ratio of instantaneous to steady-state current for HET-I<sub>Ks</sub> was also modified by the drug to a value that was not significantly different from WT-I<sub>Ks</sub> ( $p = 0.06$ , Figure 5E). These findings demonstrated the selective suppression of HET-I<sub>Ks</sub> and the normalization of this mutant current to WT-I<sub>Ks</sub> levels.

### HMR-1556 mitigates S140G-I<sub>Ks</sub>-induced atrial action potential duration shortening

We examined the effects of HMR-1556 on action potentials in cultured adult rabbit left atrial myocytes expressing WT-I<sub>Ks</sub> or S140G-I<sub>Ks</sub> channel complexes. Action potentials were elicited at 1 Hz during whole-cell current clamp recording of adenovirus transduced atrial myocytes (Figure S5). Expression of S140G-I<sub>Ks</sub> in left atrial myocytes hyperpolarized the

resting membrane potential and significantly reduced 90% action potential duration (APD<sub>90</sub>) compared to WT-I<sub>Ks</sub> expression (APD<sub>90</sub>: WT-I<sub>Ks</sub>, 177.4±21.0 msec; S140G-I<sub>Ks</sub>, 68.9±19.2 msec; p<0.001) (Figure 6A). Application of 1μM HMR-1556 did not alter APD<sub>90</sub> of WT-I<sub>Ks</sub> expressing myocytes (185.2±27.3 msec, p=0.59), whereas application of 1μM HMR-1556 significantly lengthened APD<sub>90</sub> of S140G-I<sub>Ks</sub> expressing myocytes (117.1±12.7 msec, p<0.04) (Figure 6B). These findings illustrate that HMR-1556 can selectively suppress S140G-I<sub>Ks</sub> effects on atrial action potential duration without altering action potentials in myocytes expressing WT-I<sub>Ks</sub>.

## Discussion

The discovery of mutations in familial AF illustrated the contribution of specific genetic factors to AF susceptibility and suggested molecular mechanisms for some heritable forms of this common arrhythmia. For gain-of-function KCNQ1 mutations in particular, we sought to exploit this knowledge to explore a potential targeted therapy. Specifically, we hypothesized that KCNQ1 mutations predisposing to AF encode potassium channels with distinct pharmacological properties that could render them susceptible to selective inhibition. Genotype-specific therapies for inherited arrhythmia syndromes such as congenital long-QT syndrome and catecholaminergic polymorphic ventricular tachycardia are emerging.<sup>24,25</sup> Further, a precedent for mutation-specific pharmacology of a rare, inherited disorder was established by the approval of ivacaftor for treatment of cystic fibrosis caused by CFTR-G551D.<sup>26</sup>

In this study, we investigated the utility of the selective and high affinity I<sub>Ks</sub> blocker HMR-1556 to inhibit gain-of-function KCNQ1 mutations S140G and V141M. Chromanol 293B was the first identified selective I<sub>Ks</sub> blocker, which exerts its effect at low micromolar concentrations.<sup>27</sup> The chromanol derivative HMR-1556 was developed to increase potency and improve the selectivity of I<sub>Ks</sub> inhibition.<sup>28</sup> This derivative was initially demonstrated to have an IC<sub>50</sub> of 120 nM against I<sub>Ks</sub> expressed in *Xenopus* oocytes with little effect on other recombinant potassium channels at 10 μM consistent with a high level of specificity.<sup>28</sup> In isolated canine ventricular myocytes, HMR-1556 inhibits I<sub>Ks</sub> with a nanomolar IC<sub>50</sub> whereas inhibition of other ionic currents (e.g., I<sub>Kr</sub>, I<sub>K1</sub>, I<sub>to</sub>, I<sub>Ca,L</sub>) required much higher concentrations.<sup>29</sup>

Consistent with our hypothesis, we observed that S140G-I<sub>Ks</sub> exhibits enhanced sensitivity to HMR-1556. This enhancement was correlated with the emergence of an additional high affinity state, which was also observed with V141M-I<sub>Ks</sub>. Importantly, using a concentration that predominantly inhibits the high affinity state, we demonstrated that HMR-1556 effectively suppressed HET-I<sub>Ks</sub> amplitude to a level that was not significantly different from WT-I<sub>Ks</sub>. Further, this drug concentration attenuated the use-dependent accumulation of HET-I<sub>Ks</sub> that occurs during repetitive pulsing. Importantly, we demonstrated that HMR-1556 can mitigate the S140G-I<sub>Ks</sub> induced APD shortening in cultured adult rabbit atrial myocytes without affecting action potentials in myocytes expressing WT-I<sub>Ks</sub>. These findings offer evidence supporting the potential for genotype-specific therapy of familial AF.

The potential utility of HMR-1556 or a similarly acting drug in the setting of familial AF should be considered in the context of the liabilities of inhibiting I<sub>Ks</sub> in tissues other than atria. Reduction of I<sub>Ks</sub> in ventricular muscle carries the risk of reduced repolarization reserve and predisposition to reentrant arrhythmia as in type 1 congenital long-QT syndrome. In anesthetized dogs receiving continuous intravenous infusions of HMR-1556, there was significant QTc prolongation and reproducible triggering of torsades de points with an isoproterenol bolus.<sup>30</sup> Prolongation of QTc during HMR-1556 exposure is



accentuated in dogs by co-administration of the  $I_{Kr}$  blocker dofetilide.<sup>31</sup> In Langendorff-perfused rabbit hearts, HMR-1556 alone was not sufficient to prolong monophasic action potential duration (APD) but co-administration of either dofetilide alone or dofetilide with veratridine caused significant lengthening of APD.<sup>32,33</sup> These reports emphasize the potential proarrhythmic effects of high concentration HMR-1556 or of concurrent  $I_{Ks}$  and  $I_{Kr}$  inhibition. Fortunately, our data indicate that selective inhibition of S140G- $I_{Ks}$  can be achieved at HMR-1556 concentrations that do not suppress WT- $I_{Ks}$ .

Ototoxicity is another potential concern with HMR-1556. Because  $I_{Ks}$  expressed in the stria vascularis of inner ear is important in the generation of the  $K^+$  rich cochlear endolymph, disruption of  $I_{Ks}$  has the potential to impair hearing as observed in autosomal recessive Jervell-Lange-Nielson syndrome associated with *KCNQ1* or *KCNE1* mutations.<sup>34–36</sup> Indeed, high concentrations of HMR-1556 exert a reversible ototoxicity in cats.<sup>37</sup> Again, our data suggest that there is a potential concentration range that may be free of inner ear adverse effects.

In summary, the AF-associated mutations *KCNQ1-S140G* and *KCNQ1-V141M* confer enhanced sensitivity to HMR-1556 in the context of the  $I_{Ks}$  channel complex. At a concentration that predominantly suppresses current by interacting with a novel high affinity state expressed by the S140G mutant, HMR-1556 normalized current amplitudes to levels that are not significantly different from WT- $I_{Ks}$ , and attenuated the use-dependent accumulation of current. In cultured adult rabbit atrial myocytes, HMR-1556 mitigated the shortened APD induced by S140G- $I_{Ks}$  expression. Our demonstration of selective targeting of this gain-of-function mutation provides a potential proof-of-principal for genotype-specific treatment of familial AF.

## Supplementary Material

Refer to Web version on PubMed Central for supplementary material.

## Acknowledgments

The authors acknowledge Lauren Manderfield for generating the *KCNQ1-S140G* mutation, and Richard C. Welch for assisting with isolating rabbit cardiac myocytes.

**Funding Sources:** This work was supported by Greater Southeast Affiliate Predoctoral Fellowship 11PRE7610043 from the American Heart Association, Ruth L. Kirschstein National Research Service Award for Individual Predoctoral MD/PhD Fellows F30 HL107066 from the National Heart Lung and Blood Institute (NHLBI), Public Health Service Award T32 GM07347 from National Institute for General Medical Studies for the Vanderbilt Medical-Scientist Training Program, Cooperative Research Center grant U19-HL65962-10 from NHLBI, and a Vanderbilt University Graduate School Dissertation Enhancement Grant.

## References

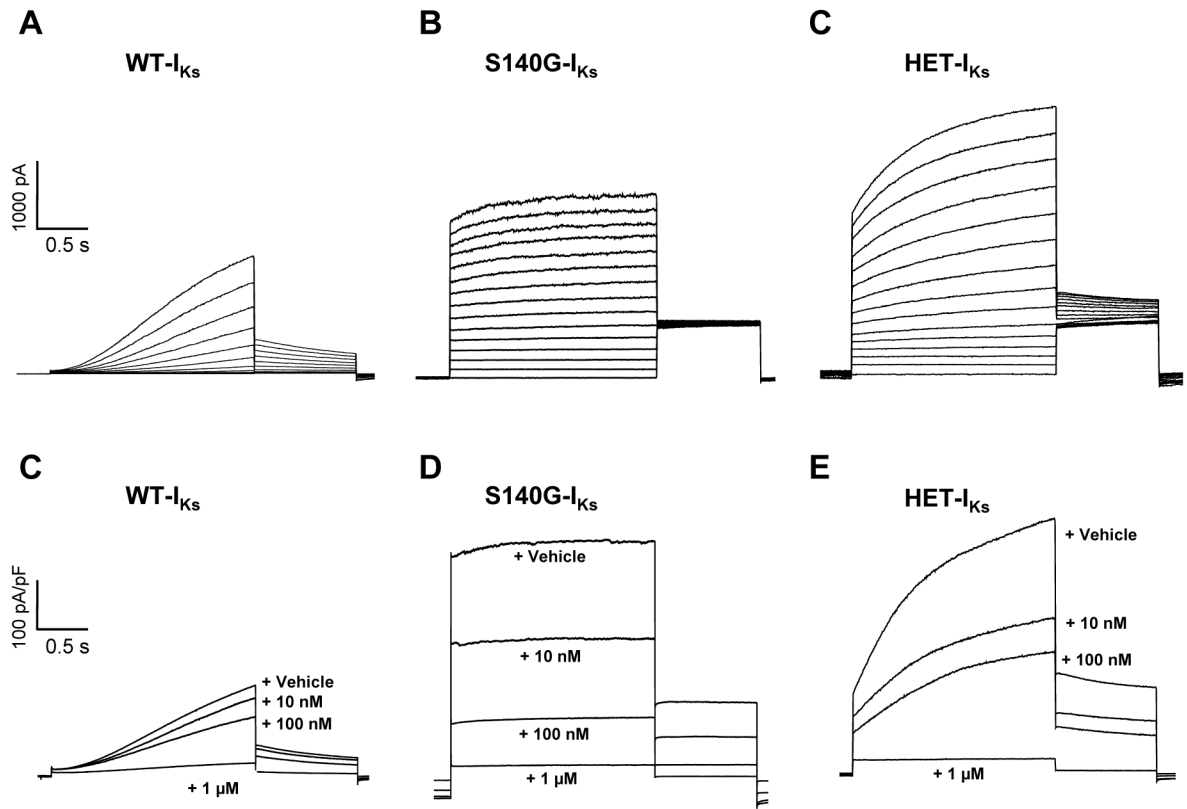
1. Go AS, Mozaffarian D, Roger VL, Benjamin EJ, Berry JD, Borden WB, Bravata DM, Dai S, Ford ES, Fox CS, Franco S, Fullerton HJ, Gillespie C, Hailpern SM, Heit JA, Howard VJ, Huffman MD, Kissela BM, Kittner SJ, Lackland DT, Lichtman JH, Lisabeth LD, Magid D, Marcus GM, Marelli A, Matchar DB, McGuire DK, Mohler ER, Moy CS, Mussolino ME, Nichol G, Paynter NP, Schreiner PJ, Sorlie PD, Stein J, Turan TN, Virani SS, Wong ND, Woo D, Turner MB. Heart disease and stroke statistics--2013 update: a report from the American Heart Association. *Circulation*. 2013; 127:e6–e245. [PubMed: 23239837]
2. Benjamin EJ, Wolf PA, D'Agostino RB, Silbershatz H, Kannel WB, Levy D. Impact of atrial fibrillation on the risk of death: the Framingham Heart Study. *Circulation*. 1998; 98:946–952. [PubMed: 9737513]

3. Kim MH, Johnston SS, Chu BC, Dalal MR, Schulman KL. Estimation of total incremental health care costs in patients with atrial fibrillation in the United States. *Circ Cardiovasc Qual Outcomes*. 2011; 4:313–320. [PubMed: 21540439]
4. Chugh SS, Blackshear JL, Shen WK, Hammill SC, Gersh BJ. Epidemiology and natural history of atrial fibrillation: clinical implications. *J Am Coll Cardiol*. 2001; 37:371–378. [PubMed: 11216949]
5. Kopecky SL, Gersh BJ, McGoon MD, Whisnant JP, Holmes DR Jr, Ilstrup DM, Frye RL. The natural history of lone atrial fibrillation. A population-based study over three decades. *N Engl J Med*. 1987; 317:669–674. [PubMed: 3627174]
6. Brand FN, Abbott RD, Kannel WB, Wolf PA. Characteristics and prognosis of lone atrial fibrillation. 30-year follow-up in the Framingham Study. *JAMA*. 1985; 254:3449–3453. [PubMed: 4068186]
7. Scardi S, Mazzone C, Pandullo C, Goldstein D, Poletti A, Humar F. Lone atrial fibrillation: prognostic differences between paroxysmal and chronic forms after 10 years of follow-up. *Am Heart J*. 1999; 137:686–691. [PubMed: 10097231]
8. Fox CS, Parise H, D'Agostino RB Sr, Lloyd-Jones DM, Vasan RS, Wang TJ, Levy D, Wolf PA, Benjamin EJ. Parental atrial fibrillation as a risk factor for atrial fibrillation in offspring. *JAMA*. 2004; 291:2851–2855. [PubMed: 15199036]
9. Gudbjartsson DF, Arnar DO, Helgadóttir A, Gretarsdóttir S, Holm H, Sigurdsson A, Jonasdóttir A, Baker A, Thorleifsson G, Kristjansson K, Pálsson A, Blondal T, Sulem P, Backman VM, Hardarson GA, Palsdóttir E, Helgason A, Sigurjonsdóttir R, Sverrisson JT, Kostulas K, Ng MC, Baum L, So WY, Wong KS, Chan JC, Furie KL, Greenberg SM, Sale M, Kelly P, MacRae CA, Smith EE, Rosand J, Hillert J, Ma RC, Ellinor PT, Thorgeirsson G, Gulcher JR, Kong A, Thorsteinsdóttir U, Stefansson K. Variants conferring risk of atrial fibrillation on chromosome 4q25. *Nature*. 2007; 448:353–357. [PubMed: 17603472]
10. Roberts R. Mechanisms of disease: Genetic mechanisms of atrial fibrillation. *Nature Clin Pract Cardiovasc Med*. 2006; 3:276–282. [PubMed: 16645668]
11. Chen YH, Xu SJ, Bendahhou S, Wang XL, Wang Y, Xu WY, Jin HW, Sun H, Su XY, Zhuang QN, Yang YQ, Li YB, Liu Y, Xu HJ, Li XF, Ma N, Mou CP, Chen Z, Barhanin J, Huang W. KCNQ1 gain-of-function mutation in familial atrial fibrillation. *Science*. 2003; 299:251–254. [PubMed: 12522251]
12. Hong K, Piper DR, Diaz-Valdecantos A, Brugada J, Oliva A, Burashnikov E, Santos-de-Soto J, Grueso-Montero J, Diaz-Enfante E, Brugada P, Sachse F, Sanguinetti MC, Brugada R. De novo KCNQ1 mutation responsible for atrial fibrillation and short QT syndrome in utero. *Cardiovasc Res*. 2005; 68:433–440. [PubMed: 16109388]
13. Olson TM, Alekseev AE, Moreau C, Liu XK, Zingman LV, Miki T, Seino S, Asirvatham SJ, Jahangir A, Terzic A.  $K_{ATP}$  channel mutation confers risk for vein of Marshall adrenergic atrial fibrillation. *Nat Clin Pract Cardiovasc Med*. 2007; 4:110–116. [PubMed: 17245405]
14. Xia M, Jin Q, Bendahhou S, He Y, Larroque MM, Chen Y, Zhou Q, Yang Y, Liu Y, Liu B, Zhu Q, Zhou Y, Lin J, Liang B, Li L, Dong X, Pan Z, Wang R, Wan H, Qiu W, Xu W, Eurlings P, Barhanin J, Chen Y. A Kir2.1 gain-of-function mutation underlies familial atrial fibrillation. *Biochem Biophys Res Commun*. 2005; 332:1012–1019. [PubMed: 15922306]
15. Yang Y, Xia M, Jin Q, Bendahhou S, Shi J, Chen Y, Liang B, Lin J, Liu Y, Liu B, Zhou Q, Zhang D, Wang R, Ma N, Su X, Niu K, Pei Y, Xu W, Chen Z, Wan H, Cui J, Barhanin J, Chen Y. Identification of a KCNE2 gain-of-function mutation in patients with familial atrial fibrillation. *Am J Hum Genet*. 2004; 75:899–905. [PubMed: 15368194]
16. Sinner MF, Pfeufer A, Akyol M, Beckmann BM, Hinterseer M, Wacker A, Perz S, Sauter W, Illig T, Nabauer M, Schmitt C, Wichmann HE, Schomig A, Steinbeck G, Meitinger T, Kaab S. The non-synonymous coding  $I_{K_r}$ -channel variant KCNH2-K897T is associated with atrial fibrillation: results from a systematic candidate gene-based analysis of KCNH2 (HERG). *Eur Heart J*. 2008; 29:907–914. [PubMed: 18222980]
17. Watanabe H, Darbar D, Kaiser DW, Jiramongkolchai K, Chopra S, Donahue BS, Kannankeril PJ, Roden DM. Mutations in sodium channel  $\beta$ 1- and  $\beta$ 2-subunits associated with atrial fibrillation. *Circ Arrhythm Electrophysiol*. 2009; 2:268–275. [PubMed: 19808477]

18. Makiyama T, Akao M, Shizuta S, Doi T, Nishiyama K, Oka Y, Ohno S, Nishio Y, Tsuji K, Itoh H, Kimura T, Kita T, Horie M. A novel SCN5A gain-of-function mutation M1875T associated with familial atrial fibrillation. *J Am Coll Cardiol*. 2008; 52:1326–1334. [PubMed: 18929244]
19. Darbar D, Kannankeril PJ, Donahue BS, Kucera G, Stubblefield T, Haines JL, George AL Jr, Roden DM. Cardiac sodium channel (SCN5A) variants associated with atrial fibrillation. *Circulation*. 2008; 117:1927–1935. [PubMed: 18378609]
20. Abraham RL, Yang T, Blair M, Roden DM, Darbar D. Augmented potassium current is a shared phenotype for two genetic defects associated with familial atrial fibrillation. *J Mol Cell Cardiol*. 2009; 48:181–190. [PubMed: 19646991]
21. Bendahhou S, Marionneau C, Haurogne K, Larroque MM, Derand R, Szuts V, Escande D, Demolombe S, Barhanin J. In vitro molecular interactions and distribution of KCNE family with KCNQ1 in the human heart. *Cardiovasc Res*. 2005; 67:529–538. [PubMed: 16039274]
22. Yang Y, Liu Y, Dong X, Kuang Y, Lin J, Su X, Peng L, Jin Q, He Y, Liu B, Pan Z, Li L, Zhu Q, Lin X, Zhou Q, Pan Q, Eurlings PM, Fei J, Wang Z, Chen YH. Human KCNQ1 S140G mutation is associated with atrioventricular blocks. *Heart Rhythm*. 2007; 4:611–618. [PubMed: 17467630]
23. Restier L, Cheng L, Sanguinetti MC. Mechanisms by which atrial fibrillation-associated mutations in the S1 domain of KCNQ1 slow deactivation of  $I_{Ks}$  channels. *J Physiol*. 2008; 586:4179–4191. [PubMed: 18599533]
24. Moss AJ, Zareba W, Schwarz KQ, Rosero S, McNitt S, Robinson JL. Ranolazine shortens repolarization in patients with sustained inward sodium current due to type-3 long-QT syndrome. *J Cardiovasc Electrophysiol*. 2008; 19:1289–1293. [PubMed: 18662191]
25. Watanabe H, Chopra N, Laver D, Hwang HS, Davies SS, Roach DE, Duff HJ, Roden DM, Wilde AA, Knollmann BC. Flecainide prevents catecholaminergic polymorphic ventricular tachycardia in mice and humans. *Nat Med*. 2009; 15:380–383. [PubMed: 19330009]
26. Ramsey BW, Davies J, McElvaney NG, Tullis E, Bell SC, Drevinek P, Griese M, McKone EF, Wainwright CE, Konstan MW, Moss R, Ratjen F, Sermet-Gaudelus I, Rowe SM, Dong Q, Rodriguez S, Yen K, Ordonez C, Elborn JS. A CFTR potentiator in patients with cystic fibrosis and the G551D mutation. *N Engl J Med*. 2011; 365:1663–1672. [PubMed: 22047557]
27. Bosch RF, Gaspo R, Busch AE, Lang HJ, Li GR, Nattel S. Effects of the chromanol 293B, a selective blocker of the slow, component of the delayed rectifier  $K^+$  current, on repolarization in human and guinea pig ventricular myocytes. *Cardiovasc Res*. 1998; 38:441–450. [PubMed: 9709405]
28. Gogelein H, Bruggemann A, Gerlach U, Brendel J, Busch AE. Inhibition of  $I_{Ks}$  channels by HMR 1556. *Naunyn Schmiedebergs Arch Pharmacol*. 2000; 362:480–488. [PubMed: 11138839]
29. Thomas GP, Gerlach U, Antzelevitch C. HMR 1556, a potent and selective blocker of slowly activating delayed rectifier potassium current. *J Cardiovasc Pharmacol*. 2003; 41:140–147. [PubMed: 12500032]
30. Gallacher DJ, Van de WA, van der LH, Hermans AN, Lu HR, Towart R, Volders PG. In vivo mechanisms precipitating torsades de pointes in a canine model of drug-induced long-QT1 syndrome. *Cardiovasc Res*. 2007; 76:247–256. [PubMed: 17669388]
31. Nakashima H, Gerlach U, Schmidt D, Nattel S. In vivo electrophysiological effects of a selective slow delayed-rectifier potassium channel blocker in anesthetized dogs: potential insights into class III actions. *Cardiovasc Res*. 2004; 61:705–714. [PubMed: 14985067]
32. So PP, Hu XD, Backx PH, Puglisi JL, Dorian P. Blockade of  $I_{Ks}$  by HMR 1556 increases the reverse rate-dependence of refractoriness prolongation by dofetilide in isolated rabbit ventricles. *Br J Pharmacol*. 2006; 148:255–263. [PubMed: 16565733]
33. So PP, Backx PH, Dorian P. Slow delayed rectifier  $K^+$  current block by HMR 1556 increases dispersion of repolarization and promotes Torsades de Pointes in rabbit ventricles. *Br J Pharmacol*. 2008; 155:1185–1194. [PubMed: 18836478]
34. Neyroud N, Tesson F, Denjoy I, Leibovici M, Donger C, Barhanin J, Fauré S, Gary F, Coumel P, Petit C, Schwartz K, Guicheney P. A novel mutation in the potassium channel gene KVLQT1 causes the Jervell and Lange-Nielsen cardioauditory syndrome. *Nat Genet*. 1997; 15:186–189. [PubMed: 9020846]

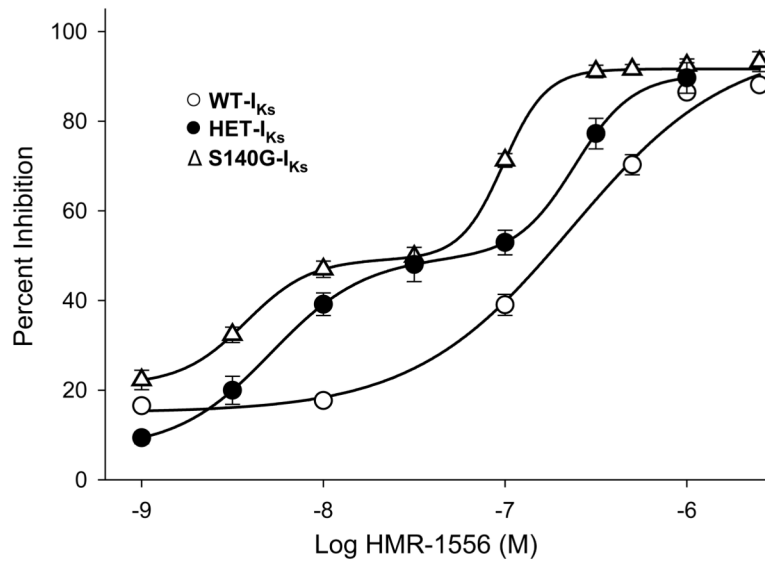


35. Tyson J, Tranebjerg L, Bellman S, Wren C, Taylor JFN, Bathen J, Aslaksen B, Sorland SJ, Lund O, Malcolm S, Pembrey M, Bhattacharya S, Bitner-Glindzicz M. IsK and KVLQT1: mutation in either of the two subunits of the slow component of the delayed rectifier potassium channel can cause Jervell and Lange-Nielsen syndrome. *Hum Mol Genet.* 1997; 6:2179–2185. [PubMed: 9328483]
36. Schulze-Bahr E, Wang Q, Wedekind H, Haverkamp W, Chen Q, Sun Y, Rubie C, Hordt M, Towbin JA, Borggreffe M, Assmann G, Qu X, Somberg JC, Breithardt G, Oberti C, Funke H. KCNE1 mutations cause Jervell and Lange-Nielsen syndrome. *Nat Genet.* 1997; 17:267–268. [PubMed: 9354783]
37. Hartmann R, Gerlach U, Klinke R. Ototoxic side-effects of the  $I_{Ks}$ -channel blocker HMR1556. *Hear Res.* 2002; 172:145–150. [PubMed: 12361877]

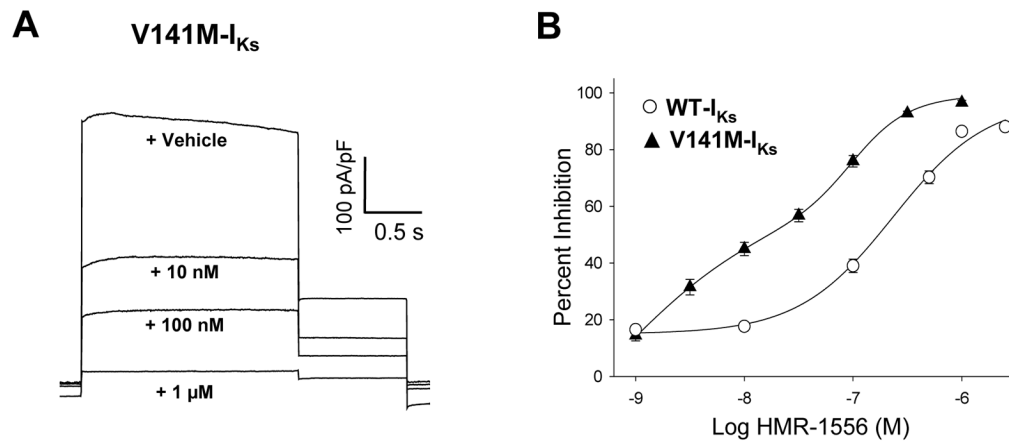


**Figure 1.**

S140G- $I_{Ks}$  and HET- $I_{Ks}$  exhibit enhanced sensitivity to HMR-1556. **A, B and C,** Representative current recordings from cells expressing WT- $I_{Ks}$  (**A**), S140G- $I_{Ks}$  (**B**), or HET- $I_{Ks}$  (**C**). Recordings illustrated in **A, B and C** were obtained using the activation protocol described in the Methods. **D, E, and F,** Average current densities (current normalized to cell capacitance) elicited by a 2 s voltage step to +40 mV followed by a 10 s interpulse during application of vehicle or various concentration of HMR-1556 from cells expressing WT- $I_{Ks}$  (**D**), S140G- $I_{Ks}$  (**E**), or HET- $I_{Ks}$  (**F**). Current density traces in **D, E, and F** are averages from 9–11 cells.

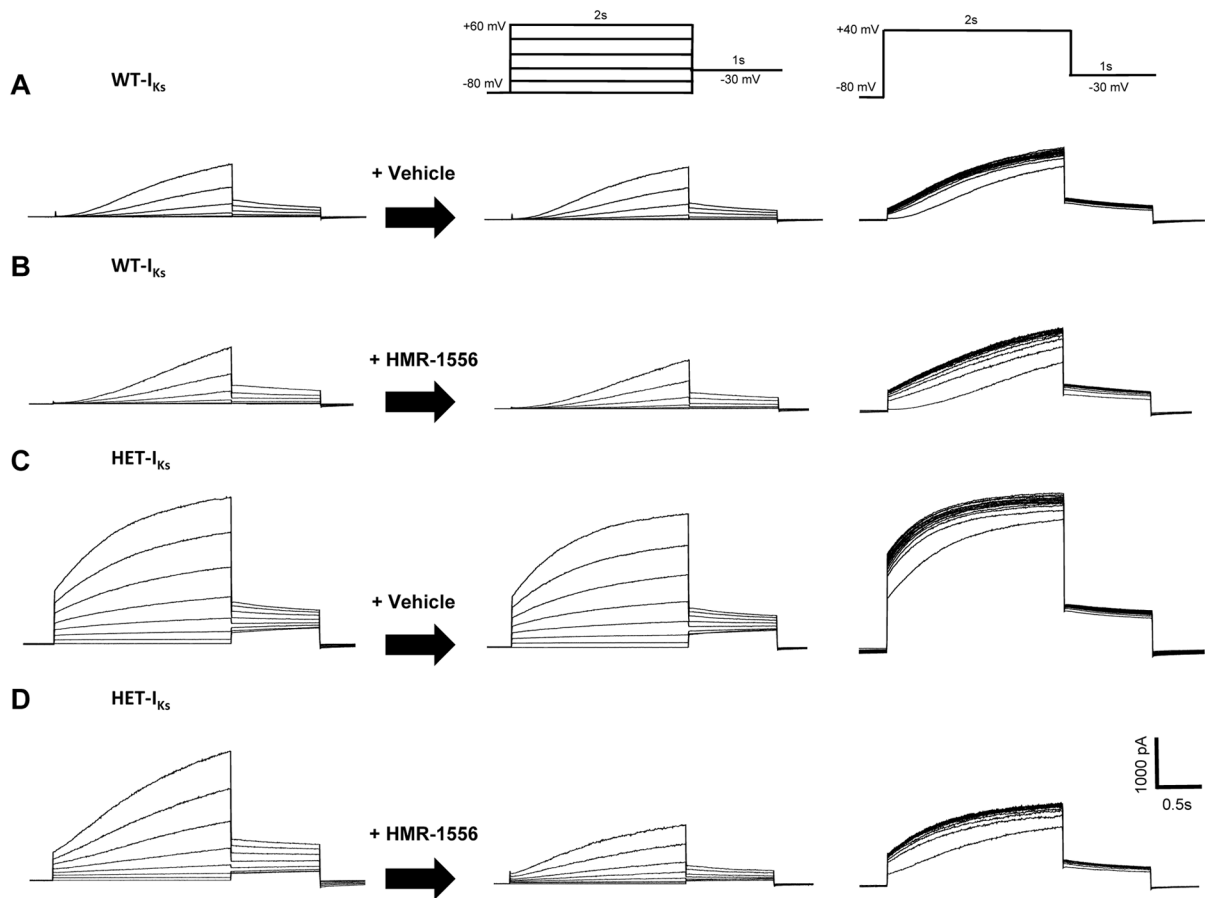


**Figure 2.** HMR-1556 concentration-response curves for WT- $I_{Ks}$  (○), S140G- $I_{Ks}$  (△), and HET- $I_{Ks}$  (●). Solid lines represent fits of the averaged data to either monophasic (WT- $I_{Ks}$ ) or biphasic (S140G- $I_{Ks}$  and HET- $I_{Ks}$ ) Hill function (see Supplemental Material).  $IC_{50}$  values and Hill coefficients are provided in the text.



**Figure 3.**

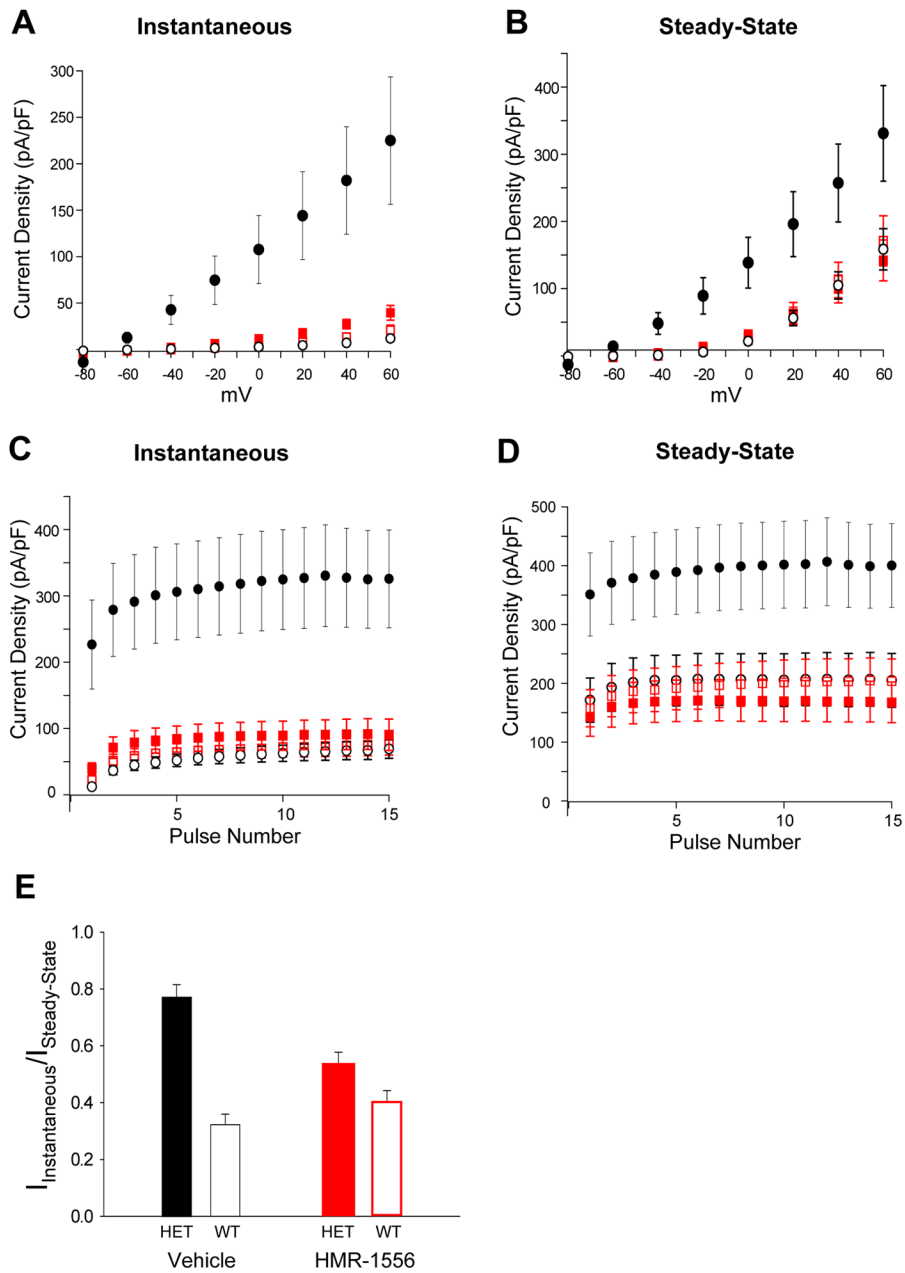
V141M-I<sub>Ks</sub> exhibits enhanced sensitivity to HMR-1556. **A**, Representative current densities (current normalized to cell capacitance) recorded from cells expressing WT-I<sub>Ks</sub> that were elicited by a 2 s voltage step to +40 mV followed by a 10 s interpulse during application of vehicle or various concentration of HMR-1556. **B**, HMR-1556 concentration-response curves for V141M-I<sub>Ks</sub> (▲) and WT-I<sub>Ks</sub> (○). Solid lines represent fits of the averaged data (9–11 cells) to a biphasic Hill function (see Supplemental Material). For V141M-I<sub>Ks</sub>, the high affinity state had an IC<sub>50</sub> of 0.72 nM and Hill coefficient of 0.6; the low affinity state had an IC<sub>50</sub> of 204 nM and Hill coefficient of 1.7.



**Figure 4.**

Selective inhibition of HET- $I_{Ks}$  by HMR-1556. **A and B**, Effects of vehicle on whole-cell currents during an activation voltage clamp protocol (middle panel) and during repetitive stimulation (right panel) from cells expressing WT- $I_{Ks}$  (**A**) or HET- $I_{Ks}$  (**B**). **C and D**, Effect of HMR-1556 (20 nM) on whole-cell currents during activation (middle panel) and repetitive stimulation (right panel) protocols from cells expressing WT- $I_{Ks}$  (**C**) or HET- $I_{Ks}$  (**D**). In **A–D**, traces in each row are from the same cell.



**Figure 5.**

Selective inhibition of HET-I<sub>Ks</sub> by HMR-1556. **A**, Voltage dependence of instantaneous current density for vehicle-treated WT-I<sub>Ks</sub> (○, n = 10), vehicle-treated HET-I<sub>Ks</sub> (●, n = 11), HMR-1556 (20 nM) treated WT-I<sub>Ks</sub> (□, n = 10), and HMR-1556 (20 nM) treated HET-I<sub>Ks</sub> (■, n = 9). Differences between vehicle-treated HET-I<sub>Ks</sub> and other groups were significant at the p<0.001 level for voltages between -20 and +60 mV. **B**, Voltage dependence of steady-state current density for vehicle or HEM-1556 treated WT-I<sub>Ks</sub> or HET-I<sub>Ks</sub> (symbols defined in A). Differences between vehicle-treated HET-I<sub>Ks</sub> and other groups were significant at the p<0.02 level for voltages between -40 and +60 mV. **C**, Use dependence of instantaneous current density for vehicle or HEM-1556 treated WT-I<sub>Ks</sub> or HET-I<sub>Ks</sub> (symbols defined in A). Differences between vehicle-treated HET-I<sub>Ks</sub> and other groups were significant at the p<0.001 level at all tested potentials. **D**, Use dependence of steady-state

current density for vehicle or HEM-1556 treated WT- $I_{Ks}$  or HET- $I_{Ks}$  (symbols defined in **A**). Differences between vehicle-treated HET- $I_{Ks}$  and other groups were significant at the  $p < 0.02$  level at all tested potentials. In **A–D**, there were no significant differences ( $p = 0.09–0.74$ ) among vehicle-treated WT- $I_{Ks}$ , HMR-1556 treated WT- $I_{Ks}$ , and HMR-1556 treated HET- $I_{Ks}$  at any voltage. **E**, Ratios of instantaneous current density to steady-state current density. Differences between vehicle-treated WT- $I_{Ks}$  (open black bar) or HET- $I_{Ks}$  (solid black bar) was significant at  $p < 0.001$ , whereas there was no significant difference ( $p = 0.06$ ) between HMR-1556 treated WT- $I_{Ks}$  (open red bar) and HET- $I_{Ks}$  (solid red bar).

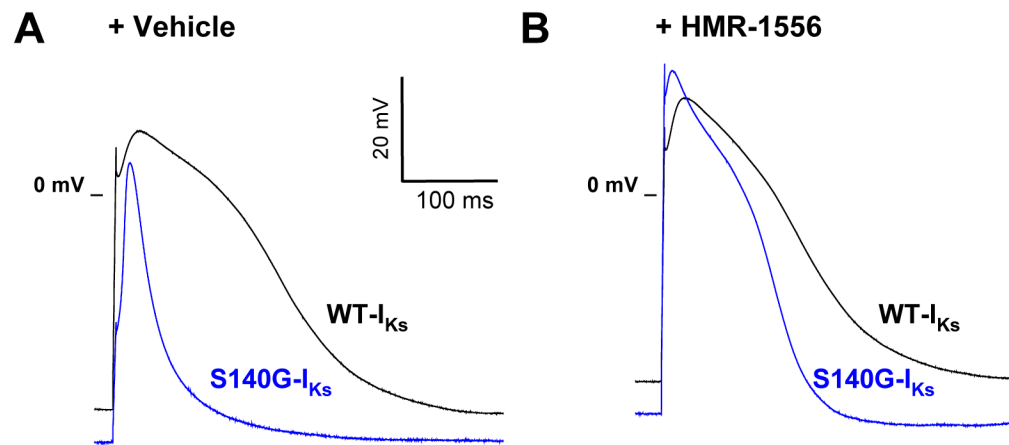


**Figure 6.** HMR-1556 mitigates atrial action potential shortening by S140G-I<sub>Ks</sub>. Representative averages of 10 sequential action potentials from cultured rabbit left atrial myocytes expressing either WT-I<sub>Ks</sub> (black line, n=6) or S140G-I<sub>Ks</sub> (blue line, n=6). **A**, Action potentials elicited after application of vehicle. **B**, Action potentials elicited after application of 1  $\mu$ M HMR-1556. APD<sub>90</sub> values are provided in the text.